NJC

Accepted Manuscript

This is an *Accepted Manuscript*, which has been through the Royal Society of Chemistry peer review process and has been accepted for publication.

Accepted Manuscripts are published online shortly after acceptance, before technical editing, formatting and proof reading. Using this free service, authors can make their results available to the community, in citable form, before we publish the edited article. We will replace this *Accepted Manuscript* with the edited and formatted *Advance Article* as soon as it is available.

You can find more information about *Accepted Manuscripts* in the Information for Authors.

Please note that technical editing may introduce minor changes to the text and/or graphics, which may alter content. The journal's standard Terms & Conditions and the Ethical guidelines still apply. In no event shall the Royal Society of Chemistry be held responsible for any errors or omissions in this *Accepted Manuscript* or any consequences arising from the use of any information it contains.

ROYAL SOCIETY OF CHEMISTRY

www.rsc.org/njc

Cite this: DOI: 10.1039/c0xx00000x

www.rsc.org/xxxxxx

ARTICLE TYPE

Reddish-orange-emitting and paramagnetic properties of $GdVO_4$: Sm^{3+}/Eu^{3+} multifunctional nanomaterials

Yanxia Liu, Guixia Liu*, Jinxian Wang, Xiangting Dong and Wensheng Yu

Received (in XXX, XXX) Xth XXXXXXXXX 20XX, Accepted Xth XXXXXXXXX 20XX
DOI: 10.1039/b000000x

A series of $GdVO_4$: Sm^{3+}, Eu^{3+} reddish-orange-emitting nanophosphors were successfully prepared by a simple one-step hydrothermal method. X-ray diffraction (XRD), field emission scanning electron microscope (FESEM), energy-dispersive X-ray spectrometer (EDS), transmission electron microscope (TEM), photoluminescence (PL) spectra, fluorescence lifetime, PL quantum-efficiency (QE) and vibrating sample magnetometer (VSM) were utilized to characterize the as-prepared samples. The results show that the individual Sm^{3+} or Eu^{3+} ions activated $GdVO_4$ phosphors exhibit excellent emission properties in their respective regions and the bright blue light from VO_4^{3-} group can be observed under the excitation of ultraviolet (313 nm). The emission intensity of Sm^{3+} singly activated $GdVO_4$ phosphors reaches the maximum when the content of Sm^{3+} is 0.025, of which the critical distance (R_{Sm-Sm}) is calculated to be 18.42 Å. Strong reddish-orange emissions can be seen in Sm^{3+} and Eu^{3+} ions co-doped $GdVO_4$ phosphors under ultraviolet light irradiation. In addition, the energy transfer phenomenon from Sm^{3+} to Eu^{3+} ions is clearly observed in $GdVO_4$: Sm^{3+}, Eu^{3+}, which is confirmed to be an electric quadrupole-quadrupole interaction and the energy transfer efficiency can reach a maximum at 92.5%. More significantly, the color becomes more saturated with the increasing of Eu^{3+} or Sm^{3+} ions content. Moreover, the as-prepared samples exhibit paramagnetic properties at room temperature. This type of multifunctional reddish-orange-emitting nanophosphor has promising applications in the fields of UV/n-UV WLEDs and biomedical science.

1 Introduction

In recent years, white light-emitting diodes (WLEDs) have been extensively investigated for their wide applications in various fields such as solid-state lighting, florescent sensors, back lights, multicolor three-dimensional display[1-2] due to their excellent high efficiency, great reliability, power saving, longer lifetime and environmentally friendly advantages[3-5]. Currently, the most commercially dominated method to obtain WLED products is to mix yellow luminescence from $Y_3Al_5O_{12}$: Ce^{3+} (YAG: Ce) phosphors with blue luminescence from LED chips[6], which offers a poor color rendering index (CRI) of 71.6 and a high correlated color temperature (CCT) of 7756 K ascribed to the deficiency of the red light, resulting that the corresponding light generated by this way is relatively cool white light, and this product is not suitable for room lighting[7-9]. So it is of great importance to develop a novel kind of reddish-orange-emitting phosphors for UV/n-UV WLEDs. Much attention has been paid to design this kind of phosphors in recent years, such as $Ba_3Lu(Gd)(PO_4)_3$: Eu^{2+}, Mn^{2+} orange-yellow-emitting phosphors[10-11], Ce^{3+}, Mn^{2+} and Eu^{2+}, Mn^{2+} doped $La_{9.33}(SiO_4)_6O_2$ orange-emitting phosphors[12] and Li-α-sialon: Eu^{3+} oxynitride phosphors[13] were investigated to be used for warm WLEDs.

The different Gd-based inorganic compounds ($GdPO_4$[14], GdF_3[15], $NaGdF_4$[16], Gd_2O_3[17], $GdVO_4$[18], etc.) have attracted great research attention because of their unique spectral properties including narrow emission bandwidths, large Stokes shifts, high luminescence efficiency, long lifetime and strong paramagnetic properties. Among all kinds of Gd-based inorganic compounds, it is accepted that tetragonal zircon type structure of $GdVO_4$ (space group I41/amd) has been demonstrated to be excellent host lattice for photoluminescence applications[19-20]. So far, most investigations have been focused on the luminescent properties of Ln^{3+} ions individually activated $GdVO_4$[21-23]. It is well known that the $^4G_{5/2}\rightarrow{}^6H_{J/2}$ (J= 5, 7, 9) characteristic emissions of Sm^{3+} ions are mainly in the orange region while Eu^{3+} ions are usually employed as activators in red-emitting phosphors due to its strong red emission and high color purity. Besides, energy transfer between activators plays an important role in realizing color-tunable emission in a single-phase host[24-25]. In addition, series of hosts such as oxynitride and nitride have been explored for obtaining red-orange-emitting phosphors other than $GdVO_4$[26-27]. So it is highly desirable to gain reddish-orange-emitting by co-incorporating Sm^{3+} and Eu^{3+} ions into $GdVO_4$ host via the energy transfer from Sm^{3+} ions to Eu^{3+} ions. Moreover, Ln^{3+} ions doped $GdVO_4$ nanocrystals can function as multifunctional materials for their promising applications in biomedical field ascribed to the high magnetic moment and isotropic electronic ground state $^8S_{7/2}$ of Gd^{3+} ions. So it is highly valuable to prepare $GdVO_4$: Sm^{3+},

Eu^{3+} nanocrystals and study their properties.

In view of the above situations, we choose $GdVO_4$ as host while Sm^{3+} and Eu^{3+} ions as activators to synthesize a series of $GdVO_4$: Sm^{3+}, Eu^{3+} nanophosphors through a simple hydrothermal method. Furthermore, we report on the structure, morphology, photoluminescence properties and the magnetic properties of the obtained phosphors. The energy transfer from host to Sm^{3+}/Eu^{3+} ions and Sm^{3+} to Eu^{3+} is also discussed in detail.

2 Experimental

2.1 Materials

All chemicals were of analytical grade and utilized as purchased without any further purification. Sodium orthovanadate dodecahydrate ($Na_3VO_4 \cdot 12H_2O$), gadolinium oxide (Gd_2O_3), europium oxide (Eu_2O_3), samarium oxide (Sm_2O_3) were purchased from Sinopharm Chemical Reagent Co., Ltd. Sodium dodecyl sulfate ($C_{12}H_{25}SO_4Na$), nitric acid (HNO_3) were purchased from Xilong Chemical Co., Ltd.

2.2 Preparation

The $Gd(NO_3)_3$, $Sm(NO_3)_3$, $Eu(NO_3)_3$ stock solutions were prepared by dissolving corresponding appropriate amounts of Gd_2O_3, Sm_2O_3, Eu_2O_3 in dilute HNO_3 (15 mol/L) under heating with agitation followed by evaporating the excess solvent. A series of rare earth ions doped $GdVO_4$ nanocrystals were synthesized by a simple hydrothermal method. A typical synthesis procedure of $GdVO_4$: 0.01 Sm^{3+}, 0.01 Eu^{3+} nanocrystals was as follows: 1mmol $RE(NO_3)_3$ [including 0.98 mmol $Gd(NO_3)_3$, 0.01mmol $Sm(NO_3)_3$ and 0.01mmol $Eu(NO_3)_3$] solutions were added into 100 mL flask containing 30 mL de-ionized water and 2 mmol $C_{12}H_{25}SO_4Na$ under vigorous stirring to form a homogeneous solution. After stirring for 1 h at room temperature, 1 mmol $Na_3VO_4 \cdot 12H_2O$ was introduced into the mixture. After additional agitation for 1 h, the homogeneous solution was transferred into a Teflon-lined stainless steel autoclave and treated for 24 h at 180 °C. When the autoclaves reached to room temperature naturally, the as-synthesized products were collected by centrifugation and washed with de-ionized water and anhydrate ethanol for several times, and dried at 80 °C for 12 h. The other samples were obtained via a similar way except for using the corresponding proper amount Ln^{3+} ions.

2.3 Characterization

XRD was examined on a Rigaku D/max-RA X-ray diffractometer with Cu Kα radiation (λ=0.15406 nm) and Ni filter, operating at 30 mA, 40 kV. Scanning speed, step length and diffraction range were 10° min^{-1}, 0.1° and 10°-90° respectively. The morphology and composition of the as-prepared samples were detected by A FEI-30 FESEM equipped with an EDS. The TEM micrographs were obtained using a JEOL JEM-2010 transmission electron microscope with a field emission gun operating at 200 kV. The excitation and emission spectra and the luminescence decay curves were obtained on a HITACHI F-7000 Fluorescence Spectrophotometer equipped with a 150 W xenon lamp as the excitation source, scanning at 1200nm/min. The quantum efficiency was obtained by a PL quantum-efficiency measurement system (C9920-02, Hamamatsu Photonics, Shizuoka) equipped with a 150 W xenon lamp. A VSM was employed to measure the magnetization of the as-obtained samples with the applied magnetic field ranging from -20 to 20 kOe. All of the measurements were carried out at room temperature.

3 Results and discussion

3.1 Phase, structure and morphology

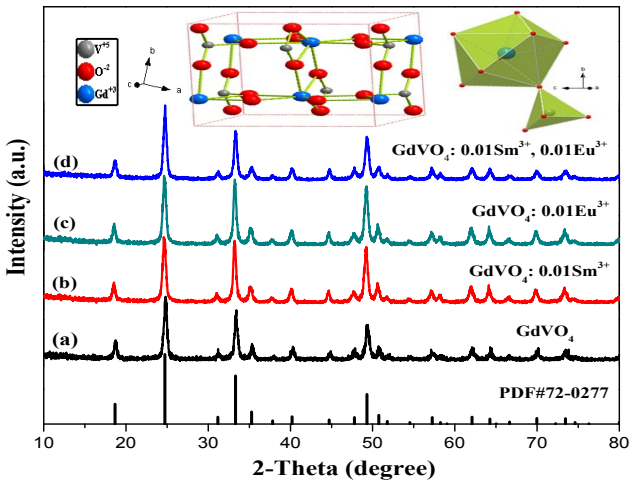

Fig. 1 XRD patterns of (a) $GdVO_4$, (b) $GdVO_4$: Sm^{3+}, (c) $GdVO_4$: Eu^{3+} and (d) $GdVO_4$: Sm^{3+}, Eu^{3+} nanocrystals. The JCPDS card 72-0277 of $GdVO_4$ is presented for comparison. The insets are schematic illustrations of tetragonal phase $GdVO_4$ structure.

The XRD patterns of the pure and Ln^{3+} ions doped $GdVO_4$ nanocrystals prepared by a facile hydrothermal method at 180 °C for 24 h were studied firstly. It can be seen that all of the diffraction peaks of pure and Ln^{3+} ions doped $GdVO_4$ can be exactly indexed into the tetragonal zircon type structure of $GdVO_4$ (JCPDS No.72-0277) with space group I41/amd, which has the cell parameters of a=b=7.19 Å, c=6.33 and Z=4. While the main peaks of Ln^{3+} ions doped $GdVO_4$ shift slightly to the lower degree compared with the corresponding standard card, this is because the ionic radius of the Sm^{3+} ions (0.964 Å) and Eu^{3+} ions (0.947 Å) are larger than that of Gd^{3+} ions (0.938 Å)[28], indicating that Sm^{3+} and Eu^{3+} ions have been successfully incorporated into $GdVO_4$ host lattice by substituting Gd^{3+} without changing the tetragonal zircon type structure of $GdVO_4$. The inset in Fig. 1 gives schematic presentation of $GdVO_4$ tetragonal structure. It can be seen that the $GdVO_4$ crystal is formed by GdO_8 polyhedron and VO_4 tetrahedron. The Gd^{3+} ions located in dodecahedral coordination are linked with eight neighboring O^{2-} ions and V^{5+} ions are tetrahedrally coordinated with O^{2-} ions[29-31].

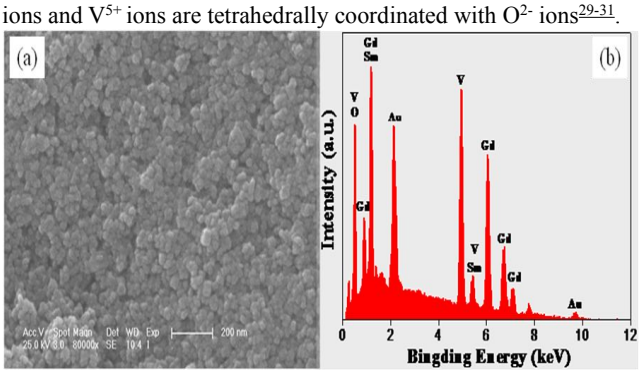

Fig. 2 (a) FE-SEM image and (b) EDS spectrum of $GdVO_4$: 0.02Sm^{3+} nanocrystals.

Fig. 2 displays the FE-SEM image and EDS spectrum of the samples obtained via a simple hydrothermal method at 180 °C for 24 h. From Fig. 2 (a), it can be discovered that the products are composed of a large number of nanoparticles and the nanoparticles are uniform in size with an average diameter of about 20-30 nm. From the EDS analysis spectrum of $GdVO_4$: $0.01Sm^{3+}$, as given in Fig. 2 (b), there are no elements can be detected other than Gd, V, O, Sm, Au (gold signals stem from spraying gold procedure), which is in good consistent with the results of the XRD.

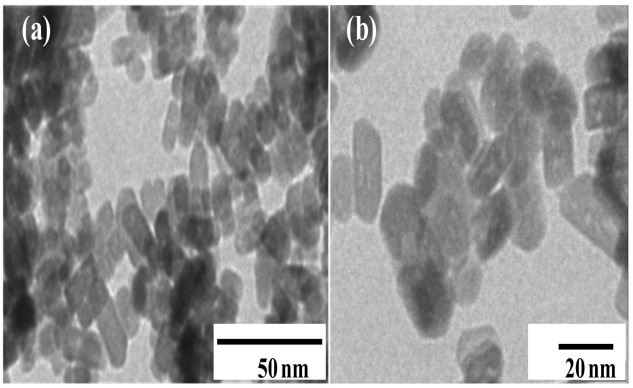

Fig. 3 (a, b) TEM images for $GdVO_4$: $0.04Sm^{3+}$ phosphors.

In order to observe clearly the morphology and size of the as-prepared samples, TEM measurement was done. Fig. 3 shows the corresponding TEM images for the as-prepared $GdVO_4$: $0.04Sm^{3+}$ phosphors. It is obvious that these particles are in short rod-like shape with the diameter of about 10 nm and length of about 20-30 nm, and the grain size was in good accordance with the results of FE-SEM.

3.2 Photoluminescence properties

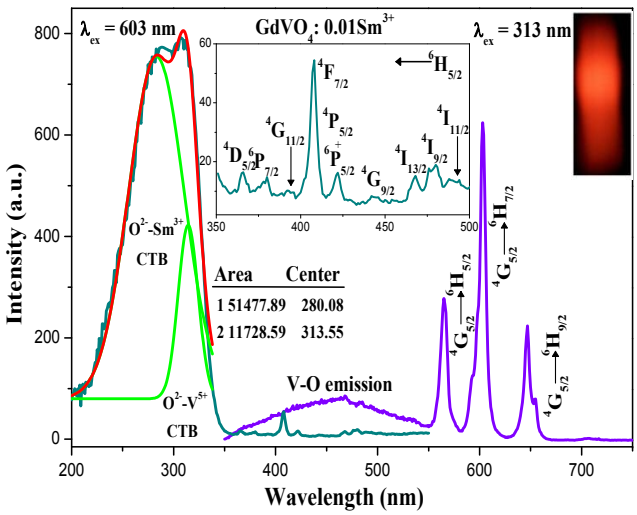

Fig. 4 Excitation and emission spectra of $GdVO_4$: $0.01Sm^{3+}$ nanocrystals. The inset is the corresponding luminescence photograph of the sample upon excitation at 313 nm.

In order to study the characteristic luminescent properties of Sm^{3+} ions in $GdVO_4$ host, Fig. 4 reveals the excitation and emission spectra of $GdVO_4$: $0.01Sm^{3+}$ nanocrystals. From the excitation spectrum monitored by the orange emission of Sm^{3+} (603 nm, $^4G_{5/2}\rightarrow{}^6H_{7/2}$), it can be observed there is a strong and broad absorption band from 200 to 350 nm which can be divided into two peaks by using Gaussian fitting. It is believed that the peaks located at approximately 280 and 313 nm are derived from O^{2-}-Sm^{3+} charge transfer (CT)[32] from oxygen 2p excited state to Sm^{3+} 4f state and O^{2-}-V^{5+} CT from oxygen 2p states to the empty d states of central vanadium in the VO_4^{3-} group, indicating that there is a strong energy migration from host to activators in tetragonal $GdVO_4$. There are some weak excitation lines in the longer wavelength region of 350-500 nm, which are originated from the intra-configurationally f-f transitions of Sm^{3+} ions from the $^6H_{5/2}$ ground state to the $^4D_{5/2}$ (363 nm), $^6P_{7/2}$ (380 nm), $^4G_{11/2}$ (394 nm), $^4F_{7/2}$ (408 nm), $^6P_{5/2}$+$^4P_{5/2}$ (422 nm), $^4G_{9/2}$ (442 nm), $^4I_{13/2}$ (468 nm), $^4I_{9/2}$ (480 nm), $^4I_{11/2}$ (494 nm) excited states, respectively. Among them, the strongest absorption is $^6H_{5/2}\rightarrow{}^4F_{7/2}$ (408 nm), which overlaps well with the typical emission wavelength of InGaN-based chips (360-470 nm)[33], implying this kind of orange-emitting phosphors can be used in n-UV WLEDs. From the emission spectrum, one can see there is a weak broad emission band centered at 470 nm (blue) ascribed to VO_4^{3-} group emission, suggesting that VO_4^{3-} group do not transfer all of the absorbed energy to Sm^{3+} ions. In addition, the f-f transitions of Sm^{3+} ions at 565, 603, 645 and 654 nm corresponding to the characteristic emissions $^4G_{5/2}\rightarrow{}^6H_{5/2}$, $^4G_{5/2}\rightarrow{}^6H_{7/2}$ and $^4G_{5/2}\rightarrow{}^6H_{9/2}$ can be discovered[34]. The photograph shows the orange emission for $GdVO_4$: Sm^{3+} phosphors upon 313 nm irradiation.

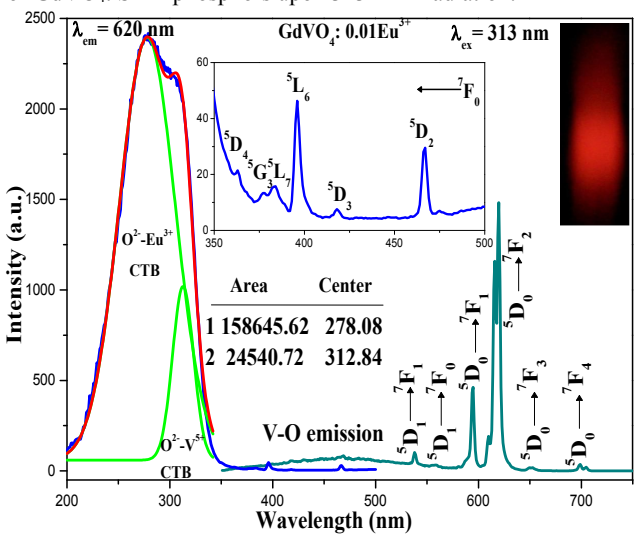

Fig. 5 Excitation and emission spectra of $GdVO_4$: $0.01Eu^{3+}$ nanocrystals. The inset is the corresponding luminescence photograph of the sample upon excitation at 313 nm.

The photoluminescence properties of Eu^{3+} ions singly activated $GdVO_4$ nanocrystals were investigated by the excitation and emission spectra of $GdVO_4$: $0.01Eu^{3+}$, which have been presented in Fig. 5. The excitation spectrum for $GdVO_4$: $0.01Eu^{3+}$ is very similar to $GdVO_4$: Sm^{3+}. Gaussian fitting confirms the strong and broad absorption band of 200-350 nm consists of two parts: the former centered at about 278 nm is the O^{2-}-Eu^{3+} CT and the latter is O^{2-}-V^{5+} CT, which corresponds to the transitions from the $^1A_2(^1T_1)$ ground state and to $^1A_1(^1E)$ and $^1E(^1T_2)$ excited state of VO_4^{3-} group in the view of molecular orbital theory[35]. Furthermore, there are some weak absorption peaks resulting from f-f transitions within the $4f^6$ configuration of the Eu^{3+} ions from the $^7F_0$ ground state to the $^5D_4$ (363 nm), $^5G_3$ (377 nm), $^5L_7$ (384 nm), $^5L_6$ (396 nm), $^5D_3$ (418 nm), $^5D_2$ (467 nm) excited states can be discovered. It can be clearly found that the f-f transitions of Eu^{3+} from 350 nm to 470 nm match well with the n-

UV LED chips. The above results indicate that $GdVO_4$: Ln^{3+} (Ln^{3+} = Sm^{3+}, Eu^{3+}) phosphors could be efficiently pumped by UV/n-UV light. Upon excitation at 313 nm, the emission spectrum exhibits a weak broad emission band and several groups of emission lines at about 537, 559, 595, 616, 620, 651 and 699 nm, which are ascribed to the $^5D_1 \rightarrow {}^7F_1$, $^5D_1 \rightarrow {}^7F_0$, $^5D_0 \rightarrow {}^7F_1$, $^5D_0 \rightarrow {}^7F_2$, $^5D_0 \rightarrow {}^7F_3$ and $^5D_0 \rightarrow {}^7F_4$ transitions for Eu^{3+} ions, respectively. The emission spectrum is dominated by the $^5D_0 \rightarrow {}^7F_2$ (616 and 620 nm) electric-dipole allowed transition of Eu^{3+}. This can be explained as in the crystalline $GdVO_4$, Gd^{3+} ions are eight-fold coordinated by O^{2-}, forming dodecahedral cages without inversion symmetry, as described in the inset of Fig. 1. When Eu^{3+} ions substitute Gd^{3+} lattice sites, non-inversion center leads to the hypersensitive electric-dipole transition of $^5D_0 \rightarrow {}^7F_2$ at 616 and 620 nm emission peaks, which is dominant in the spectrum. The photograph exhibits the reddish emission from $GdVO_4$: Eu^{3+} phosphors under the 313 nm irradiation.

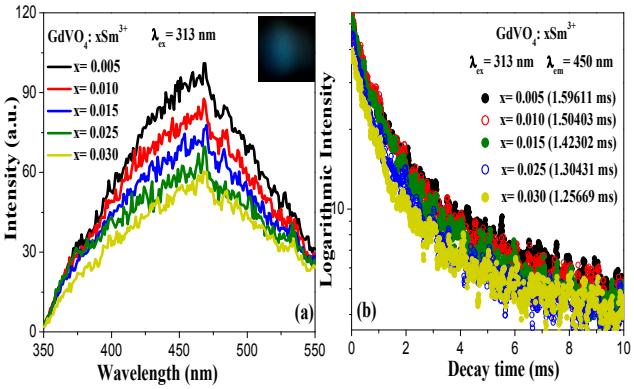

Fig. 6 PL spectra for V-O emission of $GdVO_4$: xSm^{3+} (a); decays curves of V-O emission in $GdVO_4$: xSm^{3+} nanocrystals displayed on a logarithmic intensity (excited by 313 nm and monitored by 470 nm) (b). The inset of (a) is the corresponding luminescence photograph of the sample upon excitation at 313 nm.

According to the above discussions, VO_4^{3-} group do not transfer all of the absorbed energy to Ln^{3+} ions so that the emission of V-O can be observed. In order to understand the features of V-O emission, Fig. 6 (a) exhibits the emission spectrum and the corresponding luminescent photograph of V-O emission upon 313 nm excitation. As discussed in Fig. 4 and Fig. 5, it is because the VO_4^{3-} group does not transfer the whole absorbed energy to Ln^{3+} ions in tetragonal $GdVO_4$ that in consequence a broad blue emission band originated from VO_4^{3-} group can be observed, as shown in the inset of Fig. 6 (a). The inset in Fig. 6 (a) shows the bright blue light for the V-O emission in $GdVO_4$: Sm^{3+} phosphors upon 313 nm excitation. It is worth noting that the emission intensity monotonically decreases gradually with increasing the content of Sm^{3+} due to the increasing of activators leads to VO_4^{3-} group transfer more energy to Sm^{3+} ions. The fluorescent decay curves of the VO_4^{3-} group in the $GdVO_4$: xSm^{3+} (x=0.05-0.030) samples were measured by monitoring the emission of VO_4^{3-} group at 470 nm and are exhibited in Fig. 6 (b). One can see that the decay curves can be fitted well with a single exponential function of $I=I_0+A\exp(-x/\tau)$[36] (1). The lifetimes for VO_4^{3-} group can be calculated through the above equation and discovered to decrease with the increasing of Sm^{3+} concentration, which is in accordance with the rule of the intensity.

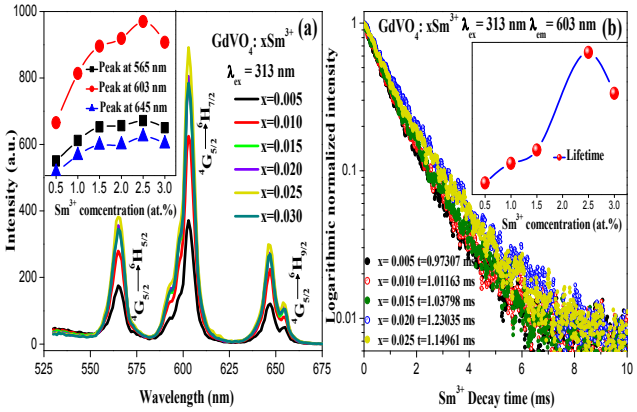

Fig. 7 Emission spectra for f-f transitions of Sm^{3+} in $GdVO_4$: xSm^{3+} upon excitation at 313 nm and the inset shows PL emission intensity of Sm^{3+} ions as a function of its concentration (a); Decay curves for the luminescence of Sm^{3+} displayed on a logarithmic intensity and the inset shows lifetime of Sm^{3+} as a function of its concentration (b).

In order to further investigate the impact of dopant concentration on the luminescence characteristics of Sm^{3+} ions, a series of $GdVO_4$: xSm^{3+} (x=0.005-0.030) nanocrystals are synthesized. Fig. 7 (a) displays the emission spectra of $GdVO_4$: xSm^{3+} , one can see that the emission intensity of Sm^{3+} increases due to the increase of luminescence centers until the Sm^{3+} concentration is above 0.025 and then decreases because of concentration quenching effect, which ascribed to the cross relaxation between neighboring Sm^{3+} ions: Sm^{3+} ($^4G_{5/2}$) + Sm^{3+} ($^6H_{5/2}$) → Sm^{3+} ($^6H_{9/2}$) + Sm^{3+} ($^6H_{9/2}$)[37]. According to Dexter's energy transfer theory[38], concentration quenching effect is mostly caused by the nonradiative energy transfer between Sm^{3+} ions at high concentration. The critical distance $R_{Sm\text{-}Sm}$ can be estimated by the following formula[39]: $R_c = 2\times[3V/(4\pi x_c Z)]^{1/3}$ (2) where V is the volume of the unit cell, x_c is the concentration of activator ions, Z stands for the number of sites that the activator ions can occupy in per unit cell. For Sm^{3+} ions singly activated $GdVO_4$, x_c is the quenching concentration that can be found to be 0.025 from the inset in Fig. 7 (a), in addition, V is 327.24 Å^3 and Z is 4. Therefore, the critical distance ($R_{Sm\text{-}Sm}$) can be calculated to be 18.42 Å, so cross relaxation will take place when the distance between Sm^{3+} ions becomes shorter than 18.42 Å. The fluorescent decay curves of the samples were measured by monitoring the strongest emission of Sm^{3+} at 603 nm (orange $^4G_{5/2} \rightarrow {}^6H_{7/2}$), as shown in Fig. 7 (b). One can see that the lifetimes for Sm^{3+} ions increase gradually until the content of Sm^{3+} is above 0.025 then decreases, which is contributed to the increase of cross relaxation rate when the distance between activators becomes shorter.

In order to study the energy transfer phenomenon between Sm^{3+} and Eu^{3+} ions in $GdVO_4$ system, Fig. 8 gives the excitation and emission spectra for $GdVO_4$: Eu^{3+}, $GdVO_4$: Sm^{3+} and $GdVO_4$: Sm^{3+}, Eu^{3+} phosphors. From Fig. 8 (a), one can see that compared with Eu^{3+} ions singly activated samples there is an obvious absorption peak at 408 nm corresponding to the $^6H_{5/2} \rightarrow {}^4F_{7/2}$ transition of Sm^{3+} ions in Sm^{3+} and Eu^{3+} ions co-doped $GdVO_4$ samples monitored by 620 nm, powerfully demonstrating that Sm^{3+} ions make a significant contribution to the emissions of Eu^{3+} ions in $GdVO_4$: Sm^{3+}, Eu^{3+} system. Furthermore, upon excitation at 408 nm, the emission intensity of Sm^{3+} ions in $GdVO_4$: Sm^{3+} significantly decreases compared to that of in

$GdVO_4$: Sm^{3+}, Eu^{3+} samples, while the emissions of Eu^{3+} at 616, 620 nm ($^5D_0 \rightarrow {}^7F_2$) can be observed, as given in Fig. 8 (b). All of these phenomena illustrate that Sm^{3+} acted as energy donors in the $GdVO_4$ host transfer excitation energy to Eu^{3+} ions served as acceptors.

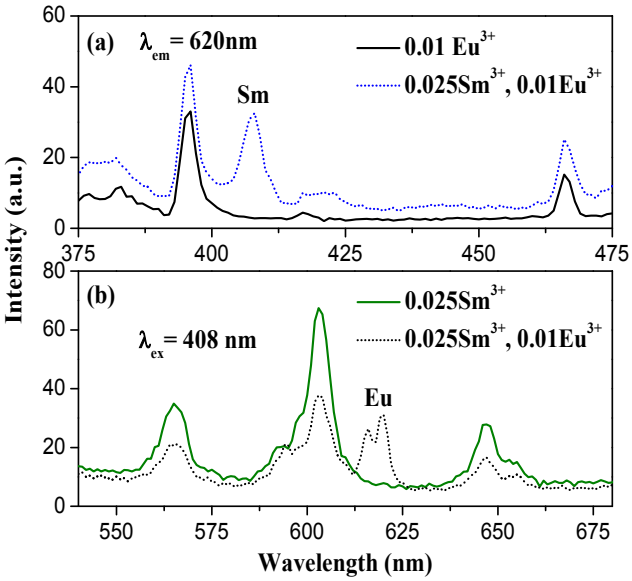

Fig. 8 (a) Excitation spectra of $GdVO_4$: $0.01Eu^{3+}$ and $GdVO_4$: $0.025Sm^{3+}$, $0.01Eu^{3+}$ nanocrystals (λ_{em}= 620 nm); (b) emission spectra of $GdVO_4$: $0.025Sm^{3+}$ and $GdVO_4$: $0.025Sm^{3+}$, $0.01Eu^{3+}$ nanocrystals (λ_{ex}= 408 nm).

In consideration of the above discussions about the luminescent properties of Sm^{3+} and Eu^{3+} ions individually doped $GdVO_4$ phosphors and the energy transfer between Sm^{3+} ions and Eu^{3+} ions, a series of Sm^{3+}, Eu^{3+} co-doped $GdVO_4$ samples fixed the Sm^{3+} content at 0.025 and varied the Eu^{3+} content from 0.00 to 0.06 have been prepared. Fig. 9 presents the variation of PL spectra and emission intensity of $GdVO_4$: 0.025 Sm^{3+}, xEu^{3+} phosphors with varying Eu^{3+} content. One can see that the intensity of Sm^{3+} ions monotonously decreases with an increase of Eu^{3+} ions doping contents while the intensity of Eu^{3+} increases gradually until the Eu^{3+} content is above 0.04 ascribed to concentration quenching: Eu^{3+} ($^5D_1$) + Eu^{3+} ($^7F_0$) → Eu^{3+} ($^5D_0$) + Eu^{3+} ($^7F_3$)[40], which occurs between the two neighboring Eu^{3+} ions. This phenomenon further supports the conclusion that Sm^{3+} acted as energy donors transfer excitation energy to Eu^{3+} ions served as acceptors in Fig. 8.

To further validate the process of energy migration from Sm^{3+} ions to Eu^{3+} ions in $GdVO_4$ system, a series of Sm^{3+}, Eu^{3+} co-doped $GdVO_4$ samples fixed the Eu^{3+} content at 0.01 and varied the Sm^{3+} content from 0.005 to 0.025 have been synthesized, as shown in Fig. 10. One can see that the red emission intensities of Eu^{3+} at 616 and 620 nm increase gradually with increasing Sm^{3+} content although the concentration of Eu^{3+} ions is fixed at 0.01 under 408 nm excitation, strongly demonstrating that there is an energy transfer from Sm^{3+} to Eu^{3+} ions that leads to the increasing for Eu^{3+} ions emission intensity. It also suggests that the color purity of Eu^{3+} ions emission can be promoted by this way and this style of red-emitting phosphors have promising applications in the fields of UV/n-UV excited WLEDs.

A decay mechanism for Sm^{3+} can be described as $1/\tau_s = /1/\tau_{so} + P_T + P_{NR}$ (3)[41] where the τ_s and τ_{so} are the lifetimes for sensitizers with and without the activator ions, P_T stands for the possibility of energy transfer from sensitizers to activators and P_{NR} presents the probability of nonradiative transitions. Assuming that all excited Sm^{3+} ions decay radiatively and substitute τ_s/τ_{so} with I_s/I_{so}, the energy transfer efficiency (η_T) from Sm^{3+} ions to Eu^{3+} ions can be calculated according to the data of intensity by the following formula $\eta_T = 1 - I_s/I_{so}$ (4)[42], where the I_s is the intensity of Sm^{3+} ions in the presence of Eu^{3+} ions and the I_{so} is the intensity of Sm^{3+} in the absence of Eu^{3+} ions. As depicted in Fig. 11 the energy transfer efficiency increases with the increasing of Eu^{3+} contents and reaches a maximum of 92.5% with the Eu^{3+} content at 0.06, implying that the energy migration from Sm^{3+} ions to Eu^{3+} ions is efficient. Moreover, the critical distance ($R_{Sm\text{-}Eu}$) in Sm^{3+} and Eu^{3+} ions co-activated $GdVO_4$ also can be estimated through the equation (2) except that the x_c is the sum content of Sm^{3+} and Eu^{3+} ions, at which the luminescence intensity of Sm^{3+} ions is half of that in the absence of $Eu^{3+}$and found to be 0.015 from the inset in Fig. 9, and the value of $R_{Sm\text{-}Eu}$ is calculated to be 21.84 Å. According to Dexter's reports[38], there are two kinds of energy transfer mechanisms which depend on the critical distance between the donor and the acceptor ions. Exchange interaction will take place when the value of R is less than 0.3-0.4 nm and there is an overlap of the donor and acceptor orbits, otherwise, the multipolar interactions may dominate. Obviously, the energy transfer from Sm^{3+} to Eu^{3+} ions in $GdVO_4$ system belongs to multipolar interactions.

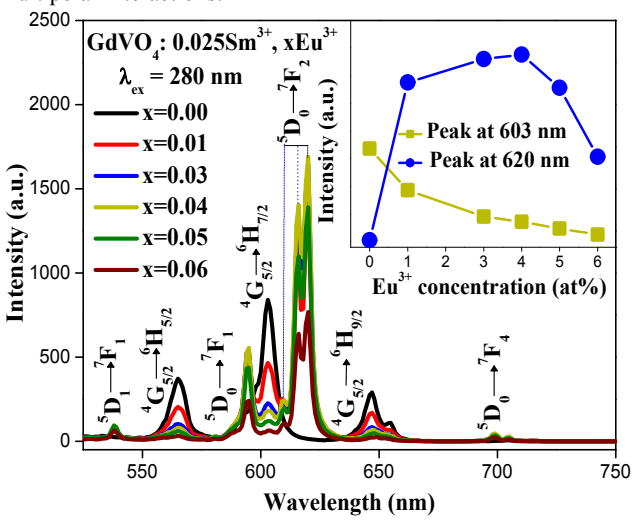

Fig. 9 Emission spectra of $GdVO_4$: $0.025Sm^{3+}$, xEu^{3+} nanocrystals (Inset is the emission intensity of Sm^{3+} and Eu^{3+} as a function of Eu^{3+} content).

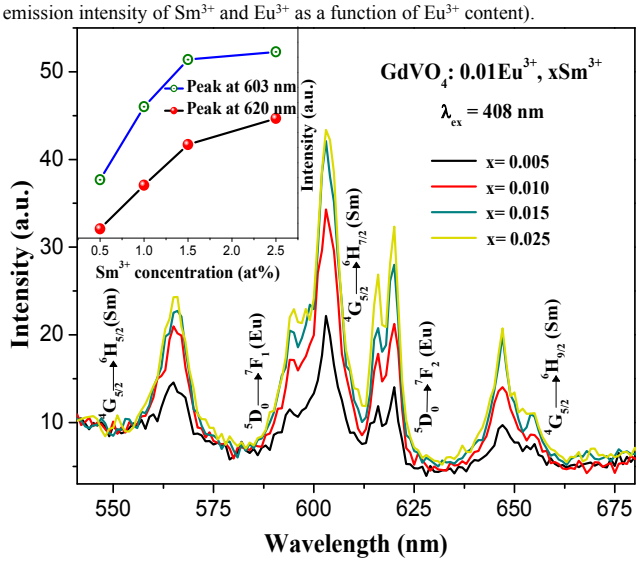

Fig. 10 Emission spectra of $GdVO_4$: xSm^{3+}, $0.01Eu^{3+}$ nanocrystals under 408 nm excitation. The inset is dependence of the emission intensity at different wavelengths on Sm^{3+} content.

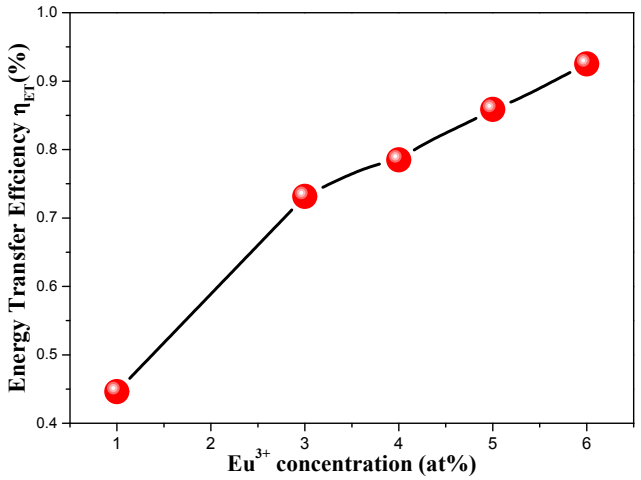

Fig. 11 Energy transfer efficiency (η_{ET}) from Sm^{3+} ions to Eu^{3+} ions in $GdVO_4$: $0.025Sm^{3+}$, xEu^{3+} nanocrystals upon 313 nm irradiation.

In order to understand the Sm^{3+}-Eu^{3+} energy transfer mechanism, the Dexter's energy transfer formula of multipolar interaction can be given as: $I_{so}/I_s \propto C^{n/3}$ (5)[36] where C is the total concentration of Sm^{3+} and Eu^{3+}, I_{so} and I_s are the corresponding emission intensities of Sm^{3+} ions without and with the presence of Eu^{3+} respectively. The plots of (I_{so}/I_s) versus $C^{n/3}$ with n=6, 8, 10 stands for dipole-dipole, dipole-quadrupole or quadrupole-quadrupole interactions, respectively. Fig. 12 exhibits the relationships between (I_{so}/I_s) and $C^{n/3}$, one can see that a liner relation is observed when n=10. This obviously indicates that the energy transfer mechanism from Sm^{3+} ions to Eu^{3+} ions is an electric quadrupole-quadrupole interaction.

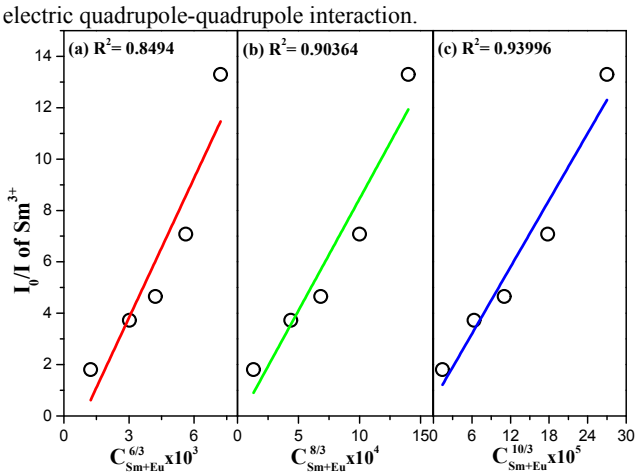

Fig. 12 Dependence of I_{so}/I_s of Sm^{3+} on (a) $C_{Sm+Eu}^{6/3} \times 10^3$, (b) $C_{Sm+Eu}^{8/3} \times 10^4$ and (c) $C_{Sm+Eu}^{10/3} \times 10^5$ in the $GdVO_4$: Sm^{3+}, xEu^{3+} nanocrystals.

According to the all above luminescence discussions, the transfer of energy in $GdVO_4$: Sm, Eu system can be depicted schematically as Fig. 13. During the excitation process, the transitions from $^1A_2(^1T_1)$ ground state of VO_4^{3-} group to $^1A_1(^1E)$ and $^1E(^1T_2)$ excited states occur and VO_4^{3-} group transfer energy to Ln^{3+} ions and emit blue light in de-excitation process. Also, electronic transitions from the O2p valence to the Sm/Eu (5d6s) conduction band take place under UV irradiation while the electrons get back to the lower energy levels once again through blue emission as well as transfer energy to Sm^{3+} and Eu^{3+} ions, the other energy is released through cross relaxation. Besides, for the emission of phonons in the $^4G_{5/2}$ energy level of Sm^{3+} ions, part of the energy can transfer to $^5D_0$ energy level of Eu^{3+} ions by electric quadrupole-quadrupole interaction and finally transfer to ^7F_J energy levels through radiative transitions.

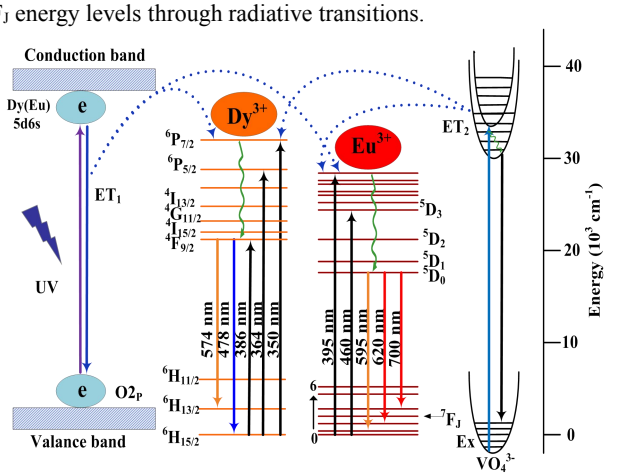

Fig. 13 The proposed schematic of energetic processes occurring in the $GdVO_4$: Sm^{3+}, Eu^{3+} samples.

The energy transfer between Sm^{3+} and Eu^{3+} ions offers an approach to increase the color purity of Eu^{3+} ions. Therefore, the CIE chromaticity coordinates for the $GdVO_4$: $0.025Sm^{3+}$, xEu^{3+} and $GdVO_4$: $0.01Eu^{3+}$, xSm^{3+} phosphors were determined based on their corresponding PL spectra. Fig. 14 exhibits the Commission International de L' Eclairage (CIE) chromaticity coordinates and the date for $GdVO_4$: $0.025Sm^{3+}$, xEu^{3+} (x=0-0.050) and $GdVO_4$: $0.01Eu^{3+}$, xSm^{3+} (x=0-0.020) nanocrystals under 313 nm radiation. It is obviously observed that $GdVO_4$: $0.025Sm^{3+}$ exhibits yellowish pink and the color gradually moves towards reddish orange region with the increasing of Eu^{3+} content, which contains more red-emitting component compared with ordinary yellow-emitting phosphors. In addition, one can see that $GdVO_4$: $0.01Eu^{3+}$ gives pink light due to the neutralization by the blue V-O emission. However, with the increasing of Sm^{3+} concentration, the color also gradually moves a redder side from pink light towards to reddish orange light and becomes more saturated. All of these results demonstrate this kind of phosphors can be used for UV/n-UV excited WLEDs. The corresponding CIE chromaticity coordinates were calculated and shown in Fig. 14 (a) and (b), respectively.

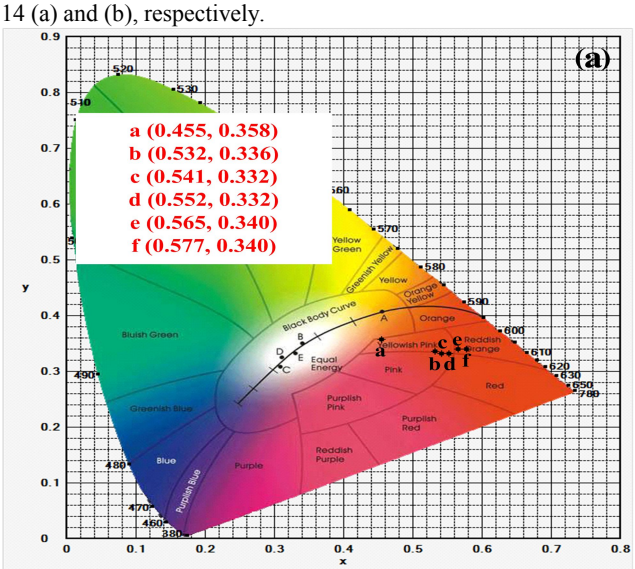

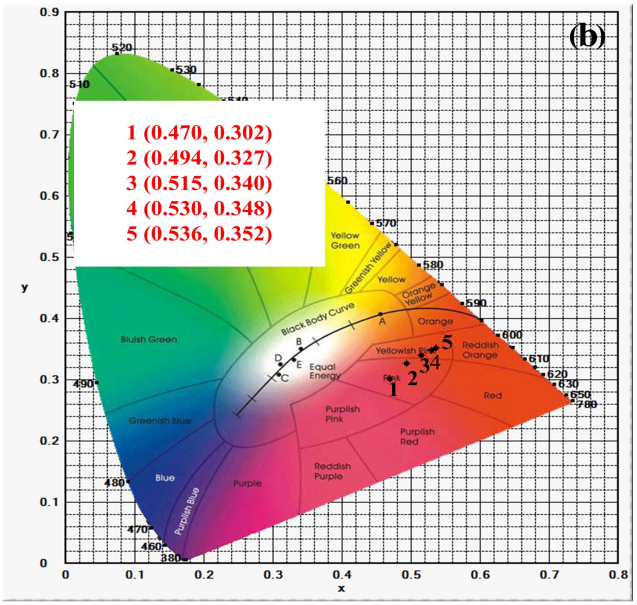

Fig. 14 CIE chromaticity diagram of (a) $GdVO_4$: $0.025Sm^{3+}$, xEu^{3+} (x= 0, 0.01, 0.02, 0.03, 0.04, 0.05); (b) $GdVO_4$: $0.01Eu^{3+}$, xSm^{3+} (x=0, 0.005, 0.01, 0.015, 0.020) under 313 nm excitation.

3.3 Quantum yield study

The quantum efficiency is an important parameter for phosphors. The luminescence quantum yields for $GdVO_4$: xSm^{3+}, $0.01Eu^{3+}$ (x= 0.005-0.025) phosphors are found to be 10.5%, 12.2%, 10.9%, 10.8% and 9.5%, respectively. These results indicate that the as-synthesized phosphors with an appropriate quantum yields and reddish-orange emission could be used for UV/n-UV WLEDs. Furthermore, the quantum efficiency can be improved by optimizing the preparation conditions and the composition of the products.

3.4 Magnetic properties

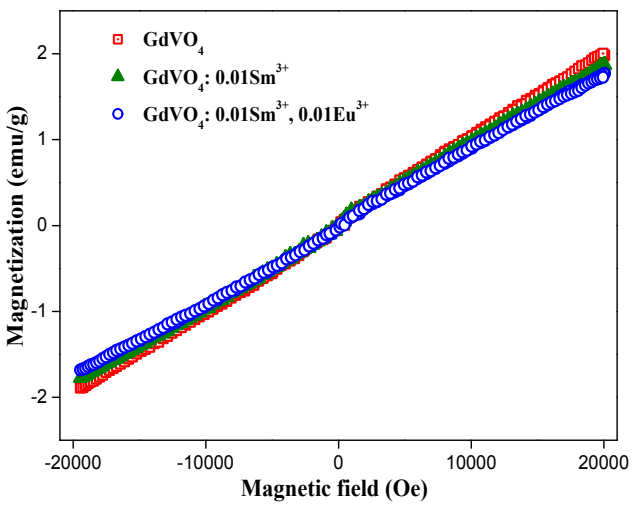

Fig. 15 Magnetization of the $GdVO_4$, $GdVO_4$: Sm^{3+}, $GdVO_4$: Sm^{3+}, Eu^{3+} nanocrystals with the increment of applied field.

In addition to the unique optical properties, the as-obtained nanocrystals exhibit magnetic properties originated from seven unpaired 4f electrons of Gd^{3+} ions. Magnetic properties of the samples were measured by using a VSM. The plot of magnetization versus applied field at room temperature is presented in Fig. 15. One can see that all of the samples show paramagnetic properties and the magnetization reaches 1.9828, 1.8698 and 1.7708 emu/g at the applied field is 20 kOe for $GdVO_4$, $GdVO_4$:$0.01Sm^{3+}$ and $GdVO_4$:$0.01Sm^{3+}$, $0.01Eu^{3+}$ nanocrystals, respectively. Compared with $GdVO_4$ nanocrystals, the magnetization of $GdVO_4$: $0.01Sm^{3+}$ and $GdVO_4$: $0.01Sm^{3+}$, $0.01Eu^{3+}$ nanocrystals decrease in sequence because Gd^{3+} ions are replaced by Sm^{3+} and Eu^{3+} ions. All of the results indicates that this kind of materials can be used for clinical medicine[43].

4 Conclusions

In summary, Sm^{3+}, Eu^{3+} co-doped nanophosphors have been prepared by hydrothermal method and the as-synthesized samples are in short rod-like shape with the diameter of about 10 nm and length of about 20-30 nm. The Sm^{3+} or Eu^{3+} ions singly activated $GdVO_4$ phosphors can efficiently absorb the ultraviolet light and emit the blue light from VO_4^{3-} group and excellent corresponding emissions originated from the f-f transitions of Sm^{3+} or Eu^{3+} ions. In the Sm^{3+} and Eu^{3+} ions co-doped $GdVO_4$ red-emitting phosphors, the energy migration from Sm^{3+} to Eu^{3+} has been verified to be an electric quadrupole-quadrupole mechanism, of which the critical distance (R_{Sm-Eu}) is estimated to be 21.84Å. Moreover, with the increasing of Eu^{3+}/Sm^{3+}concentration, the emission color gradually moves to reddish orange light and becomes more saturated. The as-obtained $GdVO_4$: Ln^{3+} (Ln^{3+} = Sm^{3+}, Eu^{3+}) nanocrystals show paramagnetic properties at room temperature. The results indicate that the as-prepared nanophosphors can be applied in the fields of UV/n-UV WLEDs and biomedical science.

Acknowledgements

This work was financially supported by the National Natural Science Foundation of P.R. China (NSFC) (Grant No. 51072026, 50972020) and the Development of science and technology plan projects of Jilin province (Grant No. 20130206002GX).

Notes and references

Key Laboratory of Applied Chemistry and Nanotechnology at Universities of Jilin Province, Changchun University of Science and Technology, Changchun, China. Fax: +86-431-85383815; Tel: +86-431-85582574; E-mail: liuguixia22@163.com

1. N. Guo, Y. Zheng, Y. Jia, H. Qiao and H. You, *New J. Chem.*, **2012**, *36,* 168-172.
2. H. A. Hoppe, *Angew. Chem. Int. Ed.*, **2009**, *48,* 3572-82.
3. S. Nakamura, T. Mukai and M. Senoh, *Appl. Phys. Lett.*, **1994**, *64,* 1687-1689.
4. Y.-S. Tang, S.-F. Hu, C. C. Lin, N. C. Bagkar and R.-S. Liu, *Appl. Phys. Lett.*, **2007**, *90,* 151108.
5. E. F. Schubert and J. K. Kim, *Science,* **2005**, *308,* 1274-1278.
6. V. Bachmann, C. Ronda and A. Meijerink, *Chem. Mater.*, **2009**, *21,* 2077-2084.
7. C. Guo, L. Luan, F. G. Shi and X. Ding, *J. Electrochem. Soc.*, **2009**, *156,* J125-J128.
8. J. Qiao, J. Zhang, X. Zhang, Z. Hao, Y. Liu and Y. Luo, *Dalton Trans.*, **2014**, *43,* 4146-4150.
9. J. Zhang, Y. He, Z. Qiu, W. Zhang, W. Zhou, L. Yu and S. Lian, *Dalton Trans.*, **2014**, *43,* 18134-18145.
10. N. Guo, Y. Huang, Y. Jia, W. Lv, Q. Zhao, W. Lu, Z. Xia and H. You, *Dalton Trans.*, **2013**, *42,* 941-947.
11. N. Guo, W. Lü, Y. Jia, W. Lv, Q. Zhao and H. You, *ChemPhysChem,*

2013, *14,* 192-197.
12. W. Lu, Y. Jia, W. Lv, Q. Zhao and H. You, *New J. Chem.,* **2013**, *37,* 3701-3705.
13. R.-J. Xie, N. Hirosaki, M. Mitomo, K. Sakuma and N. Kimura, *Appl. Phys. Lett.,* **2006**, *89,* 241103.
14. Q. Shi, F. You, S. Huang, H. Peng, Y. Huang and Y. Tao, *J. Lumin.,* **2014**, *152,* 138-141.
15. L. C. Mimun, G. Ajithkumar, M. Pokhrel, B. G. Yust, Z. G. Elliott, F. Pedraza, A. Dhanale, L. Tang, A.-L. Lin, V. P. Dravid and D. K. Sardar, *J. Mater. Chem. B,* **2013**, *1,* 5702-5710.
16. F. He, N. Niu, L. Wang, J. Xu, Y. Wang, G. Yang, S. Gai and P. Yang, *Dalton Trans.,* **2013**, *42,* 10019-10028.
17. G. Jia, K. Liu, Y. Zheng, Y. Song, M. Yang and H. You, *J. Phys. Chem. C,* **2009**, *113,* 6050-6055.
18. L. Yang, G. Li, M. Zhao, J. Zheng, D. Luo, Y. Zheng and L. Li, *Eur. J. Inorg. Chem.,* **2013**, *2013,* 5999-6008.
19. H. Xin, L.-X. Lin, J.-H. Wu and B. Yan, *J. Mater. Sci. Mater. Electron.,* 1-5.
20. N. Shanta Singh, R. S. Ningthoujam, G. Phaomei, S. D. Singh, A. Vinu and R. K. Vatsa, *Dalton Trans.,* **2012**, *41,* 4404-4412.
21. X. He, L. Zhang, G. Chen and Y. Hang, *J. Alloys Compd.,* **2009**, *467,* 366-369.
22. K. Ning, X. He, L. Zhang, Y. Liu, J. Yin, P. Zhang, G. Chen, X. Wang, Z. Chen, C. Shi, J. Hong and Y. Hang, *Opt. Mater.,* **2014**, *37,* 745-749.
23. Z. Xu, B. Feng, Y. Gao, Q. Zhao, D. Sun, X. Gao, K. Li, F. Ding and Y. Sun, *CrystEngComm,* **2012**, *14,* 5530-5538.
24. Y. Jia, W. Lu, N. Guo, W. Lu, Q. Zhao and H. You, *Phys. Chem. Chem. Phys.,* **2013**, *15,* 6057-6062.
25. Y. Liu, G. Liu, J. Wang, X. Dong and W. Yu, *Inorg. Chem.,* **2014**, *53,* 11457-11466.
26. Y. Q. Li, N. Hirosaki, R. J. Xie, T. Takeda and M. Mitomo, *Chem. Mater.,* **2008**, *20,* 6704-6714.
27. R.-J. Xie and N. Hirosaki, *Sci. Technol. Adv. Mater.,* **2007**, *8,* 588-600.
28. S. Tang, M. Huang, J. Wang, F. Yu, G. Shang and J. Wu, *J. Alloys Compd.,* **2012**, *513,* 474-480.
29. A. Szczeszak, T. Grzyb, Z. Śniadecki, N. Andrzejewska, S. Lis, M. Matczak, G. Nowaczyk, S. Jurga and B. Idzikowski, *Inorg. Chem.,* **2014**, *53,* 12243-12252.
30. L. Yang, L. Li, M. Zhao and G. Li, *Phys. Chem. Chem. Phys.,* **2012**, *14,* 9956-9965.
31. B. Shao, Q. Zhao, N. Guo, Y. Jia, W. Lv, M. Jiao, W. Lu and H. You, *CrystEngComm,* **2014**, *16,* 152-158.
32. Y. Liu, G. Liu, X. Dong, J. Wang and W. Yu, *RSC Adv.,* **2014**, *4,* 58708-58716.
33. M. Jiao, N. Guo, W. Lu, Y. Jia, W. Lv, Q. Zhao, B. Shao and H. You, *Dalton Trans.,* **2013**, *42,* 12395-12402.
34. N. S. Singh, N. K. Sahu and D. Bahadur, *J. Mater. Chem. C,* **2014**, *2,* 548-555.
35. F. He, P. Yang, D. Wang, N. Niu, S. Gai, X. Li and M. Zhang, *Dalton Trans.,* **2011**, *40,* 11023-11030.
36. L. Wu, Y. Zhang, M. Gui, P. Lu, L. Zhao, S. Tian, Y. Kong and J. Xu, *J. Mater. Chem.,* **2012**, *22,* 6463-6470.
37. M. Shang, D. Geng, X. Kang, D. Yang, Y. Zhang and J. Lin, *Inorg. Chem.,* **2012**, *51,* 11106-11116.
38. D. L. Dexter and J. H. Schulman, *J. Chem. Phys.,* **1954**, *22,* 1063-1070.
39. C. Cao, H. K. Yang, J. W. Chung, B. K. Moon, B. C. Choi, J. H. Jeong and K. H. Kim, *J. Mater. Chem.,* **2011**, *21,* 10342-10347.
40. E. Pavitra, G. S. R. Raju, Y. H. Ko and J. S. Yu, *Phys. Chem. Chem. Phys.,* **2012**, *14,* 11296-11307.
41. F. Zhang, W. Zhang, Z. Zhang, Y. Huang and Y. Tao, *J. Lumin.,* **2014**, *152,* 160-164.
42. L. Hou, S. Cui, Z. Fu, Z. Wu, X. Fu and J. H. Jeong, *Dalton Trans.,* **2014**, *43,* 5382-5392.
43. N. O. Nunez, S. Rivera, D. Alcantara, J. M. de la Fuente, J. Garcia-Sevillano and M. Ocana, *Dalton Trans.,* **2013**, *42,* 10725-10734.

Graphical Abstract

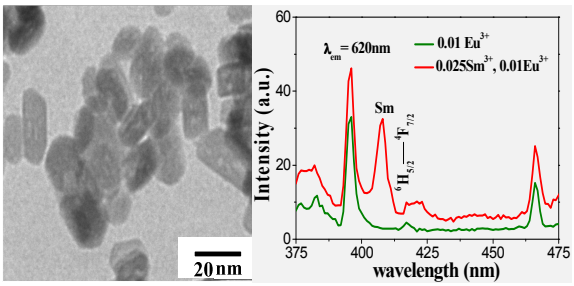

The as-prepared samples are in short rod-like shape with the diameter of about 10 nm and length of about 20-30 nm. The absorption of Sm^{3+} ions can be observed in $GdVO_4$: Sm^{3+}, Eu^{3+} samples monitored by 620 nm, indicating Sm^{3+} ions transfer energy to Eu^{3+} ions, which increases the color purity of Eu^{3+} ions in $GdVO_4$ system.